J Appl Biomed
DOI: 10.32725/jab.2025.008
journal homepage: http://jab.zsf.jcu.cz

Journal of Applied Biomedicine

Original research article

Unlocking the secrets of aortic pseudoaneurysms – exploring tensile testing of prostheses, anastomoses, and native vessels in the thoracic aorta: A clinical-engineering correlation

Sandra Rečičárová [1, 2] *, Hynek Chlup [3], Michael Jonák [1], Ivan Netuka [1]

[1] *Institute for Clinical and Experimental Medicine (IKEM), Department of Cardiovascular Surgery, Prague, Czech Republic*
[2] *Charles University, First Faculty of Medicine, Prague, Czech Republic*
[3] *Czech Technical University, Faculty of Mechanical Engineering, Laboratory of Cardiovascular Biomechanics, Prague, Czech Republic*

Abstract
Introduction: This study examines the mechanical properties of thoracic aortic false aneurysms (TAFA) and how the use of vascular prostheses, native vessels, and anastomoses affects their development. This is done through tensile testing, simulating a Bentall procedure, which is the most common surgery leading to TAFA development.
Methods: We conducted uniaxial tensile tests on the native right and left coronary arteries from five cadaveric donors. They were anastomosed to two vascular prostheses in the longitudinal and circumferential directions to assess their mechanical responses under load.
Results and discussion: All anastomosis specimens ruptured on the native vessel side, with no breaches occurring on the prosthesis side. The P2 prosthesis exhibited a mechanical response closer to that of the native vessel compared to the P1 prosthesis. There were no statistically significant differences in wall thickness or mechanical properties between the left and right coronary artery samples, leading to the merging of these groups. The strain of the anastomosis in the longitudinal direction was significantly higher than in the circumferential direction. In both directions, the strain at the onset of rupture was greater than that of the native vessel, with a particularly notable difference in the longitudinal direction. Although there was no significant difference in stress values between the longitudinal and circumferential directions, forces *per suture* were slightly higher in the circumferential direction.
Conclusion: Using the "endo-button buttress technique" with a double-layer anastomosis can help distribute the load and reduce stress. An alternative option is to use a Carrel patch to reinforce the connection between the target site and the conduit. Additionally, autologous pericardium can be employed for reinforcement.

Keywords: Aortic pseudoaneurysm; Bentall procedure; Coronary arteries; Tensile testing; Thoracic aortic false aneurysm

Highlights:
- We tested the mechanical properties of the prosthesis, native vessel, and anastomosis in both the longitudinal and circumferential directions to create an experimental model of the Bentall procedure.
- Tensile tests showed that all anastomosis specimens ruptured on the native vessel side and forces *per suture* were slightly higher in the circumferential direction.
- A specific area in the circumferential direction of the anastomosis within the native vessel has been identified as a preferred location for the formation of TAFA.

Abbreviations:
A – anastomosis; B – width; BMI – body mass index; C – circumferential direction; D – diameter of the suture fiber; DX – right coronary artery; f – failure; F – force; H – thickness; L – longitudinal direction; P – prosthesis; N – native vessel; N_s – number of sutures of the anastomosis; S – cross sections; S_d – distance between sutures; SIN – left coronary artery; TAFA – thoracic aortic false aneurysms; V – vessel

* **Corresponding author:** Sandra Rečičárová, Institute for Clinical and Experimental Medicine (IKEM), Department of Cardiovascular Surgery, Vídeňská 1958/9, 140 00 Prague, Czech Republic; e-mail: sandrarecicarova@yahoo.com
http://doi.org/10.32725/jab.2025.008
Submitted: 2025-02-10 • Accepted: 2025-05-23 • Prepublished online: 2025-06-20
J Appl Biomed 23/2: 80–90 • EISSN 1214-0287 • ISSN 1214-021X

Introduction

Acute aortic syndromes, which include aortic dissection (type A, type B, and type non-A non-B), intramural hematoma, penetrating atherosclerotic ulcer, and other conditions such as trauma or aortic pseudoaneurysm, are potentially life-threatening and require immediate evaluation and treatment. These syndromes can manifest in various ways from bleeding within the aortic wall, with different degrees of disruption that range from localized, isolated intramural hematoma to widespread, propagating medial disruption in classical aortic dissection (Czerny et al., 2024). By 1970, cystic necrosis of the media had already been documented, predominantly in older hypertensive patients (Carlson et al., 1970). Another published report shows a preference for thoracic segments and the media's inner layers (Schlatmann and Becker, 1977).

Regardless of the subtype, all acute aortic syndromes require prompt diagnosis and immediate implementation of optimal medical therapy to prevent acute complications such as organ ischemia or aortic rupture, which could lead to death. Medical treatment includes strict blood pressure management to reduce aortic wall stress, along with pain control (Czerny et al., 2024). In 1983, the adverse impact of hypertension on aortic rupture as a prognostic factor was published (Spittell, 1983). The recommended targeted systolic pressure is 100–120 mmHg, and the recommended heart rate is 60–80 bpm. It is recommended to administer intravenous beta-blockers before intravenous vasodilators (e.g., sodium nitroprusside, clevidipine) as this is effective in reducing the impulse of cardiac contraction, lowering blood pressure, and decreasing wall stress on the adventitia. Adequate invasive monitoring should be provided in an intermediate or ICU setting. The patient requires urgent cardiac surgery (Czerny et al., 2024). All of the above are known factors and recommendations in the management of acute aortic syndromes, but the evolution of the aortic false aneurysm remains unknown.

Thoracic aorta false aneurysm (TAFA) is caused by a disruption in the aortic wall, which can lead to blood leaking out and being contained by nearby structures. Although rare, this can be life-threatening and often develops from cannulation or clamping sites, aortotomy sites, or graft/coronary reimplantation sites (Razzouk et al., 1993; Rečičárová et al., 2023b). The development of these aneurysms is usually symptomatic, but they can expand over time and cause chest pain, coronary compression, dysphagia, or stridor (Dumont et al., 2004; Recicarova et al., 2024). The most common diagnosis leading to their development is aortic dissection, and the most common procedure is Bentall surgery, which consists of aortic valve replacement, ascending aorta replacement, and reimplantation of the coronary arteries. They can often be associated with connective tissue disorders (Recicarova et al., 2024). Our objective was to investigate the pathology of the origin of the thoracic aorta false aneurysm and the impact of the prosthesis, anastomosis, and native vessels on its development.

Materials and methods

Mechanical tests

From a technical point of view, we consider the vessel and the vascular prosthesis to be cylindrical vessels with circular cross-sections and a constant wall thickness. This simplification of the geometry is considered relevant (Grus et al., 2018; Rečičárová et al., 2023a; Spacek et al., 2019; Veselý et al., 2015). These structures are loaded by internal pressure, i.e., blood pressure. In a simplification where both the vessel and the vascular prosthesis are considered to be a thin-walled cylindrical shell, internal pressure generates biaxial tension in the wall (Horny et al., 2012). Anastomosis, the junction of the native vessel with the vascular prosthesis, is therefore loaded similarly. An ideal way to determine the mechanical response of the anastomosis under loading would be an inflation-extension test (Chlup et al., 2008; Grus et al., 2018; Horný et al., 2022a; Rečičárová et al., 2023a; Spacek et al., 2019). Due to the petite size of the vessel (coronary artery) and the prosthesis, this type of experiment would be very challenging to perform. The vascular prosthesis and anastomosis (suture punctures) are porous. The experiments would result in pressure medium leakage and internal pressure loss. To prevent this, it would be necessary to impregnate the inside of the anastomosis and vascular prosthesis or to insert some very thin liner through which the pressure of the fluid would act on the inner wall of the vessel-anastomosis-vascular prosthesis sample assembly. With an internal diameter of 3–4 mm, this solution would be technically difficult and would distort the data obtained. A more viscous fluid could also be used. There would be a problem with filling the sample without air bubbles. I.e., the convergence of the viscous liquid into narrow spaces.

The connection of the native vessel to the vascular prosthesis can be performed with different surgical techniques such as end-to-end, end-to-side, and side-to-side. In this research where we observed the outcomes of 112 patients with TAFA, we identified the disruption site in the coronary arteries in 18% of cases (11% in the left coronary artery site and 7% in the right coronary site), with 34% of cases having multiple disruption sites. This type of aortic surgery is known as the Bentall procedure. It is performed when there is a pathology on the aortic valve, aortic root, and ascending aorta. During this procedure, the affected structures are removed, and both the aortic valve and ascending aorta are replaced. The coronary arteries are then reimplanted to the ascending aorta replacement. We found that the Bentall procedure was the most common procedure leading to the development of TAFA, accounting for 47% of cases (Recicarova et al., 2024). Therefore, we chose to investigate the pathology of false aortic aneurysms in the simulation of the Bentall procedure.

This study focuses on the anastomosis of a native small vessel (coronary artery) to a larger vascular prosthesis (ascending aorta replacement) with the connection configuration shown in Fig. 1A. In the longitudinal and circumferential direction, see Fig. 1, Fig. 2, the native vessel and the vascular prosthesis have different mechanical properties (Chlup et al., 2008; Spacek et al., 2019; Veselý et al., 2015). The mechanical response under loading tends to be different. It is an anisotropic material. Considering the above, and in order to obtain mechanical properties in the two preferred directions, strips were separated from the vascular prosthesis in the longitudinal and circumferential directions (Fig. 2). These were joined to the coronary artery specimens using running polyproplyne sutures. Experimental specimens were created for mechanical testing of the anastomosis (Fig. 1B).

Coronary artery samples were obtained from five cadavers without any known heart or vascular disease (Table 1). The samples were anonymized according to the local legislature. For each donor, samples were always obtained from the right coronary artery (DX) and the left coronary artery (SIN). For both DX and SIN arteries, an anastomosis was created with the prosthetic vascular sample cut in both the longitudinal (SIN_1, DX_1) and circumferential (SIN_2, DX_2) directions

(Table 2, Fig. 1). For all mechanical tests, samples of the coronary arteries were excised from the aorta using the button technique. The tissue was preserved in a refrigerated saline solution at 4 °C until testing, which was conducted 24 hours after excision. The orientation of the samples was always in the longitudinal direction of the artery (Fig. 1A). A total of 20 experimental anastomosis specimens were examined. For each donor, SIN_1 and DX_1 were connected with the vascular prosthesis in the longitudinal direction and SIN_2 and DX_2 in the circumferential direction to imitate circumferential suture in the Bentall procedure. A total of 10 anastomoses in the longitudinal direction and 10 in the circumferential direction were examined (Table 2, Fig. 1). As a control group, mechanical testing was performed on four coronary arteries excised in the longitudinal direction. Two knitted crimped polyester vascular prostheses, P1 with large wavy patterns and P2 with small wavy patterns, were tested – with three samples in the longitudinal and three in the circumferential direction (Fig. 2). For the surgical procedure described above, the commercial type of vascular prosthesis is not standardized. In the Institute for Clinical and Experimental Medicine, various types of prostheses from different manufacturers are used, such as Gelweave, LeMaitre, and Goretex. For the experiments, the vascular prostheses with the smallest and largest wavy patterns were used.

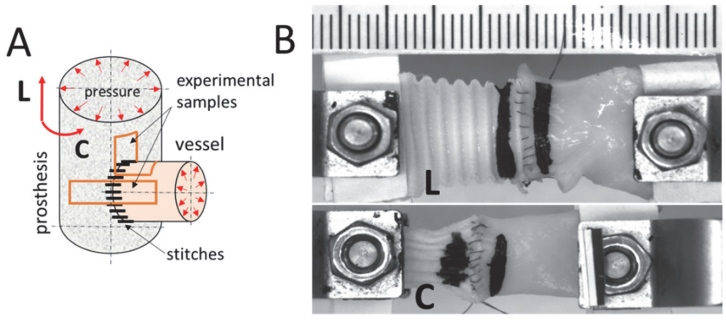

Fig. 1. Creation of an anastomosis, where **A** – connection of the native vessel to the vascular prosthesis with definition of the dominant directions L (longitudinal) and C (circumferential); **B** – demonstration of experimental samples of anastomoses in the direction L and C for the tensile test

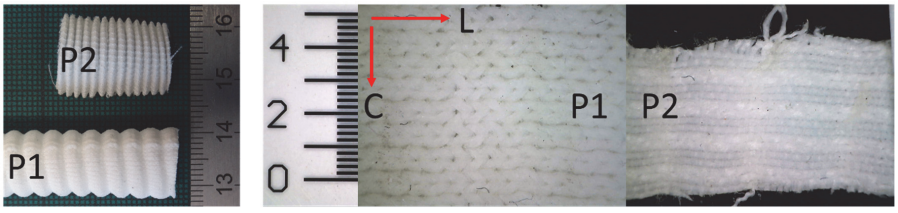

Fig. 2. The vascular prostheses used were P1 – larger wavy patterns, and P2 – smaller wavy patterns. On the right, is a detail of the wall structure (knit) of the prosthesis.

All the types of experimental samples were strip-shaped. For each experimental specimen and material type (native vessel, vascular prosthesis, anastomosis), the thickness H and width B were measured at three different locations. Thickness was measured using a Filetta digital micrometer (0–25 mm) with a modified maximum contact force of 0.5 N. For thickness measurements, the samples were sandwiched between two thin (0.2 mm) polymer transparency films. The contact pressure distribution during the measurement was ensured. The width of the samples was measured from the photographs by image analysis in NIS-Elements software.

Data on donors and dimensions of the tested samples are presented in Table 1 and Table 2. The examined anastomoses had from 8–13 sutures, i.e., an average of 10 ± 1.5 sutures. The thickness of H_A anastomoses was 1.067 ± 0.193 mm and their B_A width was 10.17 ± 1.22 mm. The distance of the stitches from each other B_{ASt} was 1.02 ± 0.15 mm. The wall thickness of the arteria coronaria H_V was 0.869 ± 0.187 mm, and the thickness of the H_P prosthesis for P1 was 0.31 ± 0.03 mm, and for P2 was 0.15 ± 0.03 mm. The sutures were made with Peters Surgical Corolene 6/0 fiber with a diameter of d = 0.06 mm by a single surgeon to standardize the technique.

Table 1. Information about blood vessel sample donors, where BMI is the calculated body mass index

Donor	Gender	Age (years)	Height (cm)	Weight (kg)	BMI
D1	M	44	179	85	26.5
D2	F	54	166	74	26.9
D3	M	29	175	69	22.5
D4	M	46	192	98	26.6
D5	M	47	180	76	23.5

Table 2. Types and basic dimensions of the tested anastomosis samples, where St – number of sutures realized in the anastomosis, A – area of all sutures for loading in the anastomosis on the side of the native vessel

Donor	Position	Thickness (mm)		Stitches	Contact area
		Vessel	Anastomosis		All stitches
		H_V	H_A	n_S (–)	A_S (mm^2)
D1	SIN_1	0.8 ± 0.06	1.182 ± 0.053	8	0.404
	SIN_2			13	0.590
	DX_1	0.715 ± 0.075	1.372 ± 0.085	13	0.609
	DX_2			10	0.390
D2	SIN_1	1.034 ± 0.171	1.071 ± 0.18	8	0.554
	SIN_2			9	0.493
	DX_1	1.082 ± 0.175	1.157 ± 0.083	8	0.587
	DX_2			9	0.507
D3	SIN_1	0.725 ± 0.037	0.782 ± 0.053	10	0.454
	SIN_2			12	0.500
	DX_1	0.695 ± 0.043	0.972 ± 0.085	12	0.480
	DX_2			10	0.434
D4	SIN_1	1.138 ± 0.022	1.246 ± 0.111	10	0.678
	SIN_2			10	0.688
	DX_1	0.934 ± 0.06	1.009 ± 0.071	10	0.587
	DX_2			10	0.534
D5	SIN_1	0.891 ± 0.079	0.978 ± 0.169	10	0.575
	SIN_2			10	0.493
	DX_1	0.677 ± 0.093	0.906 ± 0.063	10	0.457
	DX_2			10	0.356

All specimen types were loaded uniaxially in the Zwick/Roell biaxial experimental system by monotonic tension to destruction. Biological specimens are often preconditioned with 5–10 cycles of loading to a selected strain or force level. After the mechanical response has stabilized, the last cycle is analyzed (Gultova et al., 2011; Straka et al., 2017, 2018). In this study, the primary focus was on comparing the mechanical response of the anastomosis, not on analyzing the material *per se*. Therefore, simple tensile loading, such as in the works cited, was chosen as sufficient (Chlup et al., 2022, 2023; Horný et al., 2022b; Šupová et al., 2023). Here, the effect of the internal and external constraints of the material on its overall mechanical response was investigated. Cycling could lead to a gradual breaking of the bonds. In cyclic loading of biological specimens, it is usually difficult to choose a strain or force limit at which the specimen does not yet break. In biological materials, i.e., blood vessels, a large dispersion of mechanical properties is recognized (Gultova et al., 2011; Spacek et al., 2019; Straka et al., 2017, 2018; Veselý et al., 2015).

The sample was clamped between 2 clamps. Each clamp had a HBM U9C force sensor of 50 N. The strain was calculated from the displacements of the marks placed on the specimen. For anastomosis tests, the markers were placed as close to the sutures as possible, Fig. 1B. For all specimen types, markers were associated with material points on the specimen surface throughout the experiment. Marker displacement was detected by an integrated video extensometer with a resolution of 5 Mpx. The loading rate, i.e., the rate of clamp displacement, was 0.2 mm/s. Clamping of biological or soft elastic polymeric materials is usually problematic. Some options for clamping specimens for tensile testing are shown in the works cited (Chlup et al., 2022; Horný et al., 2022b; Jiang et al., 2020; Scholze et al., 2020; Šupová et al., 2023). The ends of the specimen were sandwiched between paper cartons in the clamps of the experimental system (Fig. 1B). They became more rigid, and a clamping force could be applied without the risk of damaging the experimental specimen and slipping out of the clamps during the experiment. This is similar to experiments with vascular, pericardial, or collagen gel samples (Chlup et al., 2022; Gultova et al., 2011; Straka et al., 2018; Šupová et al., 2023). Force and displacement values were recorded at 20 Hz.

To compare the different types of specimens, stress-strain relationships were obtained from the experimental data (Figs 3B, 5, 6, 7). The engineering stress, i.e., the ratio of the actual applied force F to the reference (initial) area A_S or cross-section S that transmitted the load, was used. The area of the sutures in the anastomosis transmitting the A_S load was calculated from the diameter of the suture fiber d, the vessel wall thickness H_V, and the number of realized sutures in the anastomosis n_S (schematic Fig. 3A, Table 2). The cross sections S, width multiplied by thickness, were used to calculate the stresses for the native vessel and vascular prosthesis samples. Experimental characterizations were terminated at the point onset of failure f (see schematic Fig. 3B). At this point, there is a significant shift in the characteristic directive or a significant decrease in force with increasing strain. The values of strain ε_f and stress σ_f at the onset of failure were obtained for all specimen types. To compare the mechanical response of groups of test specimens, representative average characteristics were calculated from the obtained stress-strain

relationships. A script was created in Matlab. Here, the individual groups of the $\sigma - \varepsilon$ characteristics were resampled so that the stress values of the individual characteristics could be averaged within a given group for a given deformation. Linear interpolation of the experimental data was used. Standard deviations were also obtained for each deformation state. The average characteristic can only be obtained over the region in which all specimens are subjected to the same strain.

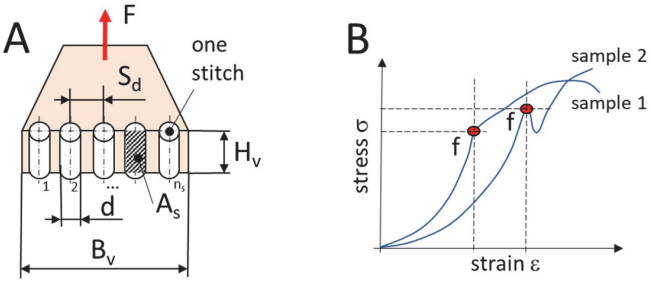

Fig. 3. Schemes for the processing of experimental data. **A** – scheme for calculating stress and area for loading (F – applied force, H_V – thickness of the vessel wall, d – diameter of the suture fiber, n_s – number of sutures of the anastomosis, S_d – distance between sutures, B_V – width of the vessel sample); **B** – scheme for identifying the point of failure onset f and obtaining stress and strain at this point.

Statistical analysis

The experimentally obtained data of measured wall thicknesses, deformations, and stresses at the detected failure initiation point f were subjected to statistical analysis. The normality of the data distribution was tested using the Shapiro–Wilk test. The non-parametric Kruskal–Wallis test with Dunn's *post hoc* test was chosen for statistical analysis. All tests were performed at a 95% significance level, $p = 0.05$. Real Statistic, an MS Excel add-in, was used for statistical analysis. Statistically significant differences between groups are indicated in the figures. Cohen's D was calculated to obtain effect size, where *** is small effect, ** is medium effect, and * is large effect. The significance limits for Cohen's D were standard, i.e., 0.2 for small, 0.5 for medium, and 0.8 for large effect.

Results

Sensorially, the vessel was more pliable than the material of the prosthesis. During mechanical testing, suture breakage was always initiated on the side of the native vessel. In order to compare the material properties of the native vessel and the vascular prostheses, mechanical tests were performed in the same manner and with the same sensors as for the anastomosis tests. The experimental planar vascular prosthesis specimens, cut in both longitudinal and circumferential directions, were never destroyed or partially broken during the test. Force sensors with a significantly higher range would be required for these tests. This would probably be beyond the construction limit of this type of experimental system. All tests were successfully conducted for the experimental samples of the native vessel and anastomoses.

Rupture of the anastomoses always occurred on the side of the vessel, consistent with our previous findings in the inflation-extension testing (Rečičárová et al., 2023a). The wall thickness and values of the tested samples were analyzed. The left and right coronary arteries were found to have similar wall thicknesses (Fig. 4A). Therefore, it was possible to merge the two groups. A group V (vessel) representing the wall thickness of the coronary artery was formed. It can be seen from Fig. 4A that the wall thicknesses of the SIN sample (left coronary artery) are slightly larger than those of the DX sample (right coronary artery). The findings align with the anatomical structure of the coronary arteries. Similarly, the anastomosis specimens examined (A) consist of the SIN (left) and DX (right) vessels. Their differences are statistically nonsignificant. The anastomosis thicknesses are similar (Fig. 4A), and were therefore merged into A. The anastomosis and vessel thicknesses were shown to be significantly different. The anastomosis has a greater thickness (Fig. 4B).

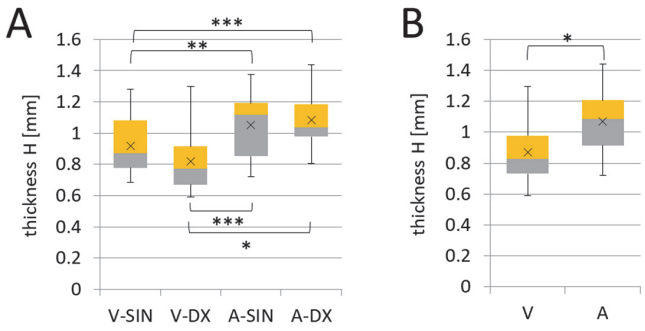

Fig. 4. Measured wall thicknesses of the tested samples. **A** – samples V (vessel) and A (anastomosis) according to the location of the left coronary artery (SIN) and right coronary artery (DX) sampling, $n = 30$; **B** – grouped measurements for V and A regardless of the location of the coronary artery, $n = 60$. Statistical differences between groups are indicated.

Mechanical stress-strain ($\sigma - \varepsilon$) characteristics were obtained for the native vessel left and right coronary arteries. The availability of biological material was challenging to obtain due to the small diameters of the vessels. Our main goal was to create and test an anastomosis which is a sutured connection between the native vessel and a vascular prosthesis. Therefore, it is not possible to compare the mechanical response of the native vessel left (SIN) and right (DX) coronary artery (Fig. 5A). As previously mentioned, biological material has a large variability in mechanical response due to e.g., gender, age, lifestyle, etc. The above measurements should be taken as indicative. From the obtained SIN and DX characteristics, the average mechanical characteristic of the coronary artery was calculated with the variance of the values (Fig. 5B). It shows the approximate range and trend of the mechanical response of the native vessel under load. As will be shown later, the $\sigma - \varepsilon$ characteristics of the native vessel are different from those of anastomoses or vascular prostheses. Even a larger number of observations would not change this.

The material of the tested vascular prostheses is stiffer than the native vessel. This is shown by the $\sigma - \varepsilon$ (Fig. 5 and Fig. 6). The higher stiffness of vascular prostheses is also typical for other types constructed from polymeric materials (Chlupáč et al., 2009; Zia et al., 2022). Some studies have investigated not only the mechanical properties of the prosthesis but also its resistance to suture breakage in anastomosis (Castillo-Cruz et al., 2019). The pliability is achieved here by the shape and construction of the prosthesis wall. Two types of used prostheses have been tested with the smallest and largest wavy patterns (Fig. 2). The wavy patterns of the vascular prosthesis are in the longitudinal direction (L) in the tested specimens. The spe-

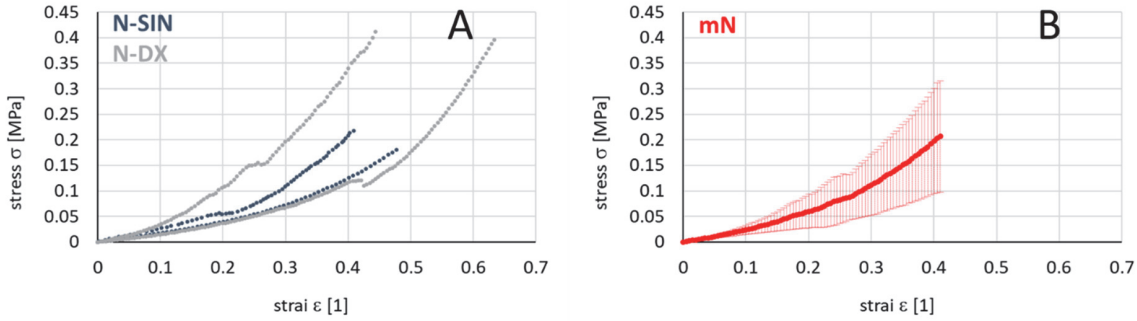

Fig. 5. Stress-strain characteristics for native (N) vessel samples cut in the longitudinal direction of the vessel. **A** – experimental characteristics of the left coronary artery (SIN) and right coronary artery (DX); **B** – mean (m) representative characteristics calculated from the experimental characteristics for native (N) vessels.

cimens are more pliable than in the circumferential direction (C). In the P2 prosthesis, which has smaller wavy patterns, the mechanical response at the beginning of loading is more affected by the straightening of the wavy patterns. At low loads, the characteristic is very flat. After straightening of the wavy patterns, the trend of the characteristic changes to very steep, i.e., very stiff (see P2-L, Fig. 6). From the experimental characteristics, representative average characteristics were calculated with indicated data scatter (Fig. 6B). Due to prostheses from the opposite spectrum, i.e., small and large wavy patterns with different wall construction, the theoretical mechanical response of the virtual average prosthesis was calculated from the obtained characteristics (Fig. 6A). The stress-strain characteristics of the virtual average prosthesis in the circumferential and longitudinal directions, with the deviations indicated, are shown in Fig. 6C.

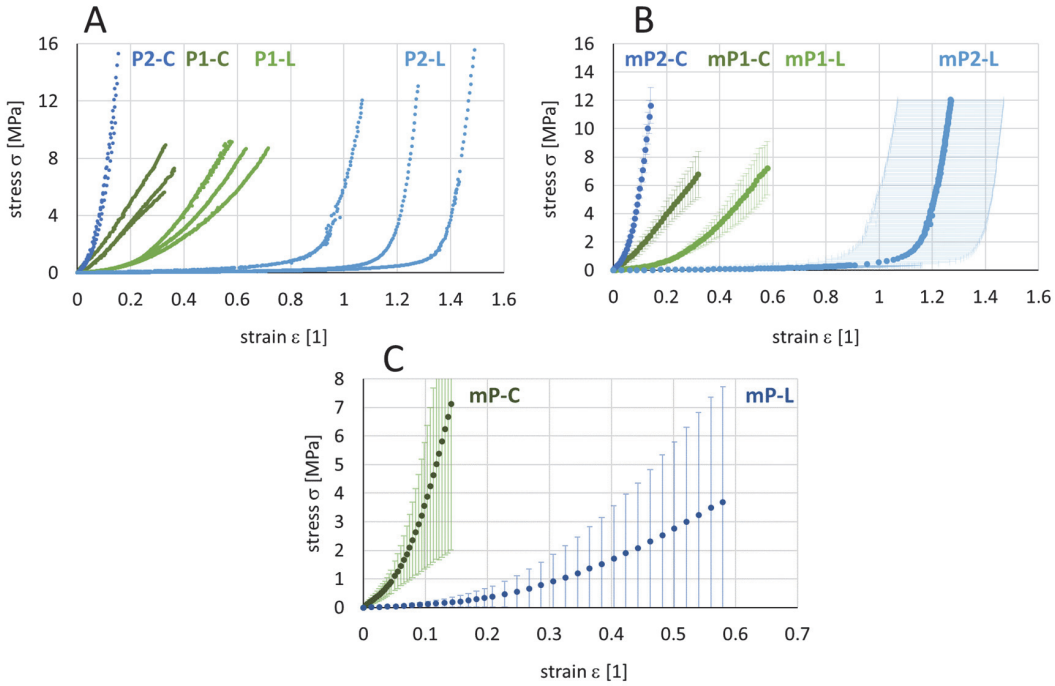

Fig. 6. Stress-strain characteristics for samples of two different vascular prostheses (P1, P2). **A** – experimental characteristics of P1 and P2 vascular prosthesis samples cut from tubular geometry in the longitudinal (l) and circumferential (C) directions, Fig. 2; **B** – average (m) representative characteristics for vascular prostheses P1 and P2 calculated from experimental characteristics; **C** – average (m) representative characteristics in the L and C directions for virtual (theoretical) vascular prosthesis P calculated from experimental characteristics of P1 and P2 in the L and C directions.

The experimental stress-strain characteristics for the created anastomoses of the native vessel with the vascular prosthesis in the longitudinal and circumferential directions are shown in Fig. 7A, B. It is difficult to identify different mechanical properties for anastomoses formed with P1 and P2 prostheses. The $\sigma - \varepsilon$ characteristics for the P1 and P2 prostheses have more scatter and overlap. This is probably a consequence of the good placement of the deformation tracking markers. These were in the immediate vicinity of the anastomosis, Fig. 1B. This means that we are primarily monitoring the mechanical response of the anastomosis with minimal influence from the remaining native vessel and prosthesis material. A change in the steepness of the $\sigma - \varepsilon$ characteristics for the L and C directions can be discerned. The data were grouped according

to the L and C direction. The type of prosthesis P1 and P2 were not taken into account (Fig. 7C). The average characteristics with standard deviations were obtained from the data. They represent the mechanical response of the anastomosis in the L and C direction (Fig. 7D). The mechanical response of the anastomosis in the C-direction is steeper than in the L-direction. Under the same load, the anastomosis deforms less in the C-direction than in the L-direction. The mechanical response of the anastomosis is an integration of the material properties of the native vascular wall, sutures, and the wall of the vascular prosthesis. If we assume that the sutures and suture material are the same, then the material of the native vessel wall and the prosthesis, which is part of the anastomosis, influence this behaviour. The material of the native vessel can only be influenced with great difficulty. The material and wall structure of the prosthesis can be better modified.

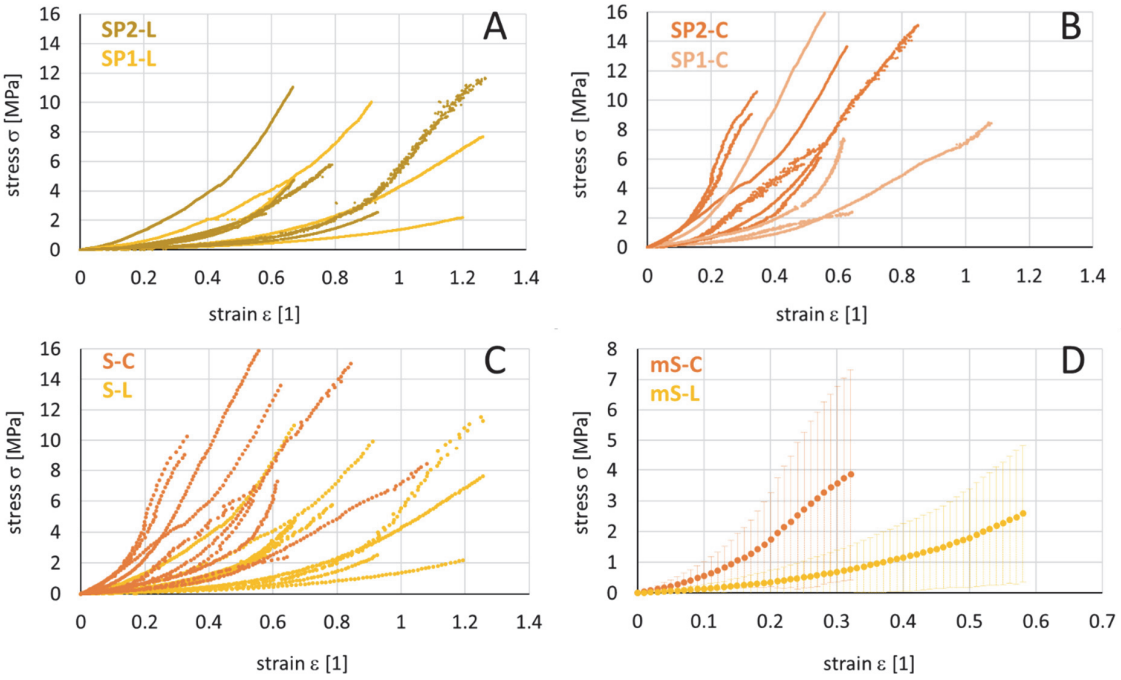

Fig. 7. Stress-strain characteristics for the anastomosis samples studied, **A** – experimental characteristics of suture samples (S, anastomoses) of the native vessel, with prosthesis samples P1 and P2 cut in the longitudinal direction (L); **B** – experimental characteristics of suture samples (S, anastomoses) of the native vessel, with prosthesis samples P1 and P2 cut in the circumferential direction (C); **C** – grouped characteristics from arrays A and B according to the orientation direction (C, L) regardless of the type of prosthesis; **D** – average (m) representative characteristics of the anastomosis (S) calculated from the experimental characteristics of array C, i.e., connection of the native vessel with the virtual (theoretical) vascular prosthesis P for the C and L directions.

The calculated average characteristics from the experimental data are shown in Fig. 8. The average characteristics represent the trend of the mechanical response of the tested group of samples. In Fig. 8, they are shown on the scale of the graph chosen according to the mechanical characteristics of the native vessel. The characteristic of the prosthesis P2 in the longitudinal direction (mP2-L) is closest to the native vessel (mN) (Fig. 8A). If we compare this characteristic with the characteristics in Fig. 6A, B, we can say that in this loading region, the wavy patterns of the prosthesis are straightened. The dominant factor influencing the mechanical response of the prosthesis is the change in the geometric shape of the wall. For the P1 prosthesis, the load transfer mechanism will be similar to that of P2. However, the wall material structure here will engage in the longitudinal direction earlier. According to Fig. 6A, B, this strain can be estimated to be from 0.25–0.30. From this limit, the characteristics of P1 in the L and C directions have a very similar slope. Similarly, this limit for the P2 prosthesis in the L direction is about 1.15 strain. All the characteristics in the longitudinal direction, both prosthesis and anastomosis, are closer to the mechanical response of the vessel wall (Fig. 8). The mechanical characteristic of the native vessel is closest to the mechanical characteristic of the anastomosis formed by the prosthesis in the longitudinal direction, mS-L. The mS-L characteristic is similar to the stress-strain relationship of the average virtual prosthesis in the longitudinal direction, mP-L (Fig. 8B). It averages both the wavy patterns P1 and P2 and the wall material structure.

The experimental data was used to evaluate the limit state. For each experimental sample, the f-point of failure onset was identified. At this point, the values of strain ε_f and stress a σ_f were obtained. These are shown for the anastomosis and native vessel samples in Figs 9 and 10.

Using statistical analysis, it was found that there is no statistically significant difference in the values of strain or stress at point f between the anastomosis formed by the left coronary artery (SIN) and the right coronary artery (DX). This is true for both the L and C directions (see Figs 9A, 10A). Thus, it does not matter whether the anastomosis in the L or C orientation is formed at the SIN or DX. From the graphs in Figs 9 and 10 it can be observed that the SIN specimens, in both L and C directions, achieved higher strain values and lower stress values than the DX anastomosis specimens. However, these differences are statistically insignificant in the given measurement range.

We merge the SIN and DX samples and focus only on the anastomosis orientation (Figs 9B and 10B). Here we see that the anastomosis samples in the C direction (S-C) achieve sim-

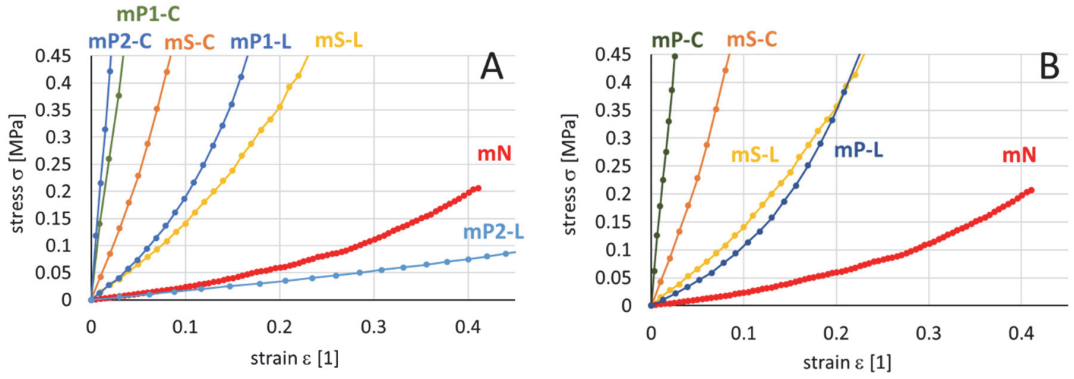

Fig. 8. Detail of the average representative stress-strain characteristics for all types of specimens studied. **A** – native vessel (mN), both types of vascular prostheses P1 and P2 loaded in the L and C directions, average anastomosis characteristics (mS) realized in the L and C directions; **B** – comparison of the characteristics of the virtual (theoretical) prosthesis (mP) with the anastomosis (mS) and native vessel (mN) in the L and C directions, see Figs 1, 2.

ilar strain but much higher stress than the native N arteria coronaria vessel. In the L direction, the anastomosis was more compliant. Higher strains were achieved as in the N samples. Stress was lower than in the C direction but still significantly higher than the native N vessel.

For the point of failure onset, the force per suture in the anastomosis in the L and C directions was calculated from the experimental data (Fig. 10C). It was calculated with the number of sutures in the anastomosis and the fact that there is no statistically significant difference between the wall thickness of the sample vessel. There was also no difference in the thickness of the anastomosis (Fig. 4A). There was no statistical difference in the forces per stitch in the anastomosis F_f between the L and C directions. They are slightly higher in the C direction (Fig. 10C). Forces per suture in the L direction are 0.305 ± 0.158 N, and in the C direction 0.471 ± 0.260 N.

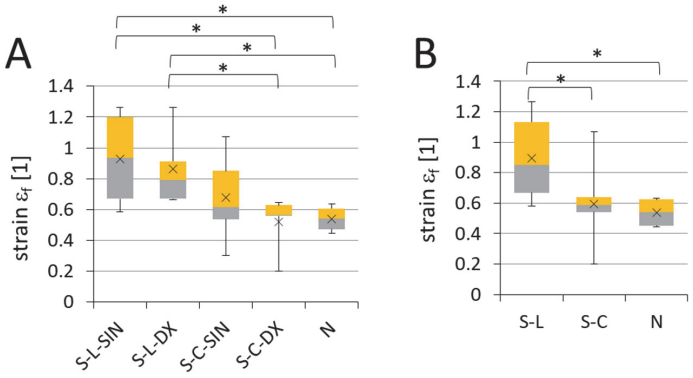

Fig. 9. Strain values at the point of failure onset f, obtained from the stress-strain characteristics, comparing the native vessel (N) with **A** – values of anastomoses (S) in the L and C direction for the SIN and DX artery locations, n = 5; **B** – values of anastomoses (S) in the L and C direction, SIN and DX locations together, n = 10 (Fig. 7C).

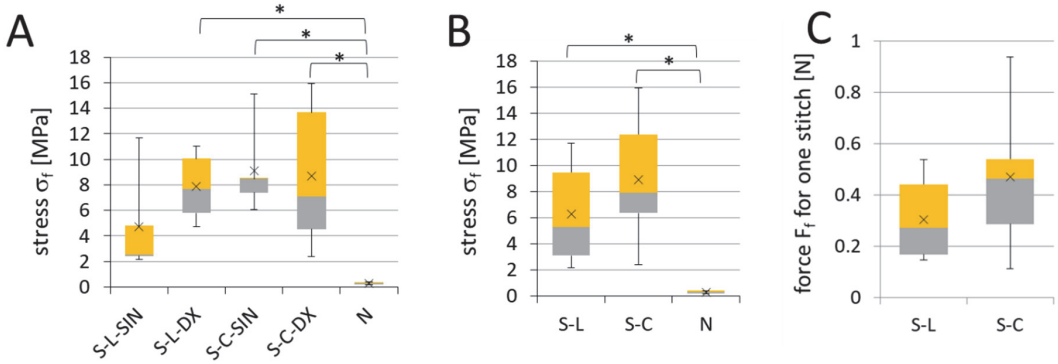

Fig. 10. Stress and force values at point f obtained from stress-strain characteristics comparing the native vessel (N) with **A** – values of anastomoses (S) in the L and C directions for the SIN and DX artery locations, n = 5; **B** – values of anastomoses (S) in the L and C directions when SIN and DX locations are merged, n = 10 (Fig. 7C); **C** – force exerted *per suture* in the anastomosis on the native vessel side calculated from experimental data, n = 10.

Discussion

Our objective was to design a reproducible model that would examine the mechanical properties of the anastomosis between a sutured coronary artery and a prosthesis. This model aims to elucidate why Bentall surgery is the most common procedure associated with the development of thoracic aortic false aneurysm when the coronary arteries are detached from the prosthesis.

The use of tissue glue causes doubts in the literature about the possible formation of thoracic aortic false aneurysms. Some studies have published their concerns, including possible transmigration of glue across suture holes, distal embolization, and false aneurysm or anastomotic disruption (Durmuş et al., 2015; Kobayashi et al., 2018; Rubio Alvarez et al., 2011).

On the contrary, other publications refute the suspicion of an association with the formation of false aneurysms (Fehrenbacher and Siderys, 2006; Ma et al., 2017). One publication even suggests a positive effect of tissue glue, which induces inflammatory changes, and according to their analysis, increased inflammation and vascularisation might even stabilize the aortic wall (Witter et al., 2010).

Many studies have used tensile testing on human tissue such as the aorta (Dong et al., 2022; Duprey et al., 2016; Fukui et al., 2005; García-Herrera et al., 2012; Petuchova et al., 2023; Sugita and Matsumoto, 2013; Takada et al., 2023) or coronary arteries (Claes et al., 2010; Karimi et al., 2013, 2015). The objectives of the studies are varied, but regardless of the goal and experimental method, the results depend on the conditions under which the tests are carried out. To our knowledge, no studies have used this type of testing on three specimens: coronary arteries as native vessels, anastomosis, and prosthesis.

Several studies have used uniaxial tensile tests *in vitro* to assess the mechanical properties of soft tissues (Sugita and Matsumoto, 2013). However, *in vivo*, aortic tissues experience biaxial stretching in both longitudinal and circumferential directions due to blood pressure and axial tethering. This suggests that biaxial stretch tests are a more appropriate method for evaluating the mechanical properties of aortic tissues. Elastic properties of aneurysmal tissues obtained through biaxial tensile testing have been reported (Fukui et al., 2005).

In conventional biaxial tensile tests, the specimen is held in place using threads. In this setup, cracks can easily form at the hooked areas due to the concentration of stress at those points. As a result, it becomes challenging to stretch the specimens until they rupture under these conditions (Duprey et al., 2016).

We used an equibiaxial tensile test system capable of stretching specimens until they rupture, allowing us to observe the microscopic deformation of the samples. All tested specimens were successfully stretched until failure. These techniques allowed us to closely examine the crack initiation process, helping us to understand the events occurring at the crack initiation site in the coronary arteries.

Loading of the specimens was to destruction, except for the vascular prosthesis specimens due to reaching the force limits of the experimental system. All anastomosis specimens began to rupture on the native vessel side during loading. No breaches ever occurred on the prosthesis side. In the P2 prosthesis, after initial straightening of the wavy patterns, the trend of the characteristic changes to very steep, i.e., very stiff (see P2-L, Fig. 6). In the P1 prosthesis, the mechanical response is similar in both longitudinal and circumferential directions. The native vessel specimens were significantly more pliable and had a flatter stress-strain characteristic than the tested anastomoses or prosthesis material. This was true for the longitudinal and circumferential directions chosen. In the range of strain up to approx. 0.4 (i.e., deformation of 40%), which corresponds to the deformation of the native vessel, the anastomosis specimens formed by the prosthesis P2 in the longitudinal direction mS-L were closest to the mechanical response of the native vessel mN (Fig. 8B). To the best of our knowledge, no studies have compared the outcomes of different vascular prostheses in tensile testing.

Published articles on tensile testing of coronary arteries did not address the differences between the right and left coronary arteries (Claes et al., 2010; Karimi et al., 2013, 2015). In our study, although the mean thickness in the left coronary artery was a bit larger than in the right coronary artery (Fig. 4), there were no statistically significant differences in wall thickness or mechanical properties between the left (SIN) and right (DX) coronary artery samples, leading to the merging of these groups.

The mechanical response of the anastomosis includes the properties of the native vessel, the geometry (design) of the sutures, the properties of the fibers, and the properties of the prosthesis wall. The focus of the anastomosis was on the orientation of the vascular prosthesis, as well as the longitudinal and circumferential directions. The strain of the anastomosis in the L direction was statistically significantly different – higher than in the C direction. In both directions, the strain of the studied anastomoses at the onset of rupture was higher than that of the native vessel. In the C direction, the strain was similar to that of the native vessel. In the L direction, the anastomosis achieved approximately 1.5 times the strain of the native vessel (Fig. 9).

The stresses at the point of failure onset were significantly different between the native vessel and anastomosis samples in both directions (Fig. 10B). These high stresses and stress concentrations in the suture area will cause the vessel wall material to breach and progressively cut through the sutures. There was no statistically significant difference between the stress values σ_f v in the L and C directions, but higher values were obtained in the C direction. The calculated forces *per suture* were also slightly higher in the C direction, but no statistical difference was found between the L and C directions. The circumferential direction may be more susceptible to complications like an aortic false aneurysm due to higher stress concentrations. Our findings disagree with another study that did not find a significant difference between circumferential and longitudinal specimens (García-Herrera et al., 2012).

In cases where the target tissue quality is poor, the "endo-button buttress technique" with a two-layer anastomosis can be used. This approach helps distribute the load and minimize stress on the tissue. The technique was first described in 2000 by Pratali et al.

Another lesser-known modification, described by Kawazoe in 1993, is the use of a Carrel patch to reinforce the connection between the target and the conduit. According to Hashimoto, another variant involves the use of autologous pericardium (Pratali et al., 2000).

Conclusion

We successfully created a model of and experimental specimen of a coronary artery – anastomosis – prosthesis to test their mechanical properties which can be reproduced. The mechan-

ical properties of anastomosis in the coronary arteries from five human cadavers and the corresponding prosthesis were studied using *in vitro* tensile testing until failure. Although the number of patients is limited, and a broader sample of arteries from individuals of different ages should be examined for more comprehensive conclusions, the initial results could be significant in understanding the causes of thoracic aortic false aneurysm formation.

The impact of the prosthesis

Tensile tests showed that all anastomosis specimens ruptured on the native vessel side, with no breaches occurring on the prosthesis side. In the P1 prosthesis, the initial straightening period is shorter, which then leads to stiffening; the mechanical response is similar in both longitudinal and circumferential directions. In the P2 prosthesis, after the initial straightening of the wavy patterns, the stiffness of the material increases significantly. The anastomosis specimens created with the P2 prosthesis in the longitudinal direction (mS-L) closely resemble the mechanical response of the native vessel (mN) when deformed by 40%, which corresponds to the deformation typically observed in a native vessel.

The P2 prosthesis exhibited a mechanical response closer to that of the native vessel compared to the P1 prosthesis.

The impact of the left or right coronary artery

There were no statistically significant differences in wall thickness or mechanical properties between the left (SIN) and right (DX) coronary artery samples, leading to the merging of these groups.

The impact of the anastomosis

The study found that in both directions the strain at the onset of rupture was greater than that of the native vessel, with a particularly notable difference in the longitudinal direction. High stresses in the suture area of the anastomosis could lead to failure. Although there was no significant difference in stress values between the longitudinal and circumferential directions, forces *per suture* were slightly higher in the circumferential direction. Consequently, the findings indicate that the circumferential direction is more prone to developing initial breakage.

In cases where the target tissue quality is poor, the "endo-button buttress technique" with a two-layer anastomosis can be used. This approach helps distribute the load and minimize stress on the tissue. The technique was first described in 2000 by Pratali et al.

Another lesser-known modification, described by Kawazoe in 1993, is the use of a Carrel patch to reinforce the connection between the target and the conduit. According to Hashimoto, another variant involves the use of autologous pericardium.

The flexibility of the anastomosis is crucial, and this depends on the surgeon's careful assessment of tissue quality. By evaluating the tissues properly, the surgeon can optimize both the number of stitches and the mechanical integrity of the anastomosis.

In conclusion, understanding the mechanical interactions at the anastomosis can inform surgical practices to reduce the risk of TAFA development, highlighting the importance of prosthesis selection and suturing techniques in improving patient outcomes.

Ethical committee

The aortic and coronary artery tissues were retrieved from the deceased, and the tensile tests were conducted within 48 hours. This protocol was approved by the Ethics Committee of the Institute for Clinical and Experimental Medicine and the Thomayer University Hospital, Prague, Czech Republic (protocol code: 24702/22, G-22-39; date of approval: September 14, 2022).

Funding

Funded by the project National Institute for Research of Metabolic and Cardiovascular Diseases (Programme EXCELES, Project No. LX22NPO5104) – Funded by the European Union – Next Generation EU.

This study was supported by project grants awarded by the Ministry of Health of the Czech Republic no. NW24-02-00206 and NW24-08-00133.

Conflict of interest

The authors have no competing interests to declare.

References

Carlson RG, Lillehei CW, Edwards JE (1970). Cystic medial necrosis of the ascending aorta in relation to age and hypertension. Am J Cardiol 25(4): 411–415. DOI: 10.1016/0002-9149(70)90006-8.

Castillo-Cruz O, Avilés F, Vargas-Coronado R, Cauich-Rodríguez JV, Cha-Chan LH, Sessini V, Peponi L (2019). Mechanical properties of l-lysine based segmented polyurethane vascular grafts and their shape memory potential. Mater Sci Eng C 102: 887–895. DOI: 10.1016/j.msec.2019.04.073.

Chlup H, Horny L, Zitny R, Konvickova S, Adamek T (2008). Constitutive Equations for Human Saphenous Vein Coronary Artery Bypass Graft. Int J Med Health Biomed Bioeng Pharm Eng 2(8): 272–275.

Chlup H, Skočilas J, Štancl J, Houška M, Žitný R (2022). Effects of Extrusion and Irradiation on the Mechanical Properties of a Water-Collagen Solution. Polymers (Basel) 14(3): 578. DOI: 10.3390/polym14030578.

Chlup H, Suchý T, Šupová M (2023). The electron beam induced cross-linking of bovine collagen gels with various concentrations: The mechanical properties and secondary structure. Polymer (Guildf) 287: 126423. DOI: 10.1016/j.polymer.2023.126423.

Chlupáč J, Filová E, Bačáková L (2009). Blood vessel replacement: 50 years of development and tissue engineering paradigms in vascular surgery. Physiol Res 58 Suppl 2: S119–S140. DOI: 10.33549/physiolres.931918.

Claes E, Atienza JM, Guinea GV, Rojo FJ, Bernal JM, Revuelta JM, Elices M (2010). Mechanical properties of human coronary arteries. 2010 Annual International Conference of the IEEE Engineering in Medicine and Biology. Buenos Aires, Argentina, pp. 3792–3795. DOI: 10.1109/IEMBS.2010.5627560.

Czerny M, Grabenwöger M, Berger T, Aboyans V, Della Corte A, Chen EP, et al. (2024). EACTS/STS Guidelines for Diagnosing and Treating Acute and Chronic Syndromes of the Aortic Organ. Ann Thorac Surg 118(1): 5–115. DOI: 10.1016/j.athoracsur.2024.01.021.

Dong H, Liu M, Lou X, Leshnower BG, Sun W, Ziganshin BA, et al. (2022). Ultimate tensile strength and biaxial stress–strain responses of aortic tissues – A clinical-engineering correlation. Appl Eng Sci 10: 100101. DOI: 10.1016/j.apples.2022.100101.

Dumont E, Carrier M, Cartier R, Pellerin M, Poirier N, Bouchard D, Perrault LP (2004). Repair of aortic false aneurysm using deep hypothermia and circulatory arrest. Ann Thorac Surg 78(1): 117–120; discussion 120–121. DOI: 10.1016/j.athoracsur.2004.01.028.

Duprey A, Trabelsi O, Vola M, Favre JP, Avril S (2016). Biaxial rupture properties of ascending thoracic aortic aneurysms. Acta Biomater 42: 273–285. DOI: 10.1016/j.actbio.2016.06.028.

Durmuş E, Kıvrak T, Sunbul M, Ataş H, Ak K, Sarı I, Tigen K (2015). Pseudoaneurysm formation due to bioglue use in aortic valve surgery. Eur J Ther 21(4): 256–258. DOI: 10.5578/GMJ.10817.

Fehrenbacher J, Siderys H (2006). Use of BioGlue in Aortic Surgery: Proper Application Techniques and Results in 92 Patients. Heart Surg Forum 9(5): E794–E799. DOI: 10.1532/HSF98.20061066.

Fukui T, Matsumoto T, Tanaka T, Ohashi T, Kumagai K, Akimoto H, et al. (2005). *In vivo* mechanical properties of thoracic aortic aneurysmal wall estimated from *in vitro* biaxial tensile test. Biomed Mater Eng 15(4): 295–305.

García-Herrera CM, Atienza JM, Rojo FJ, Claes E, Guinea GV, Celentano DJ, et al. (2012). Mechanical behaviour and rupture of normal and pathological human ascending aortic wall. Med Biol Eng Comput 50(6): 559–566. DOI: 10.1007/s11517-012-0876-x.

Grus T, Lambert L, Mlcek M, Chlup H, Honsova E, Spacek M, et al. (2018). *In Vivo* Evaluation of Short-Term Performance of New Three-Layer Collagen-Based Vascular Graft Designed for Low-Flow Peripheral Vascular Reconstructions. Biomed Res Int 2018: 3519596. DOI: 10.1155/2018/3519596.

Gultova E, Horny L, Chlup H, Zitny R (2011). A comparison between the exponential and limiting fiber extensibility pseudo-elastic model for the mullins effect in arterial tissue. J Theor Appl Mech 49(4): 1203–1216.

Horný L, Chlup H, Kužma J, Růžička P (2022a). Inflation-extension behaviour of 3D printed elastomer tubes and their constitutive description. Bioprinting 25: e00192. DOI: 10.1016/j.bprint.2022.e00192.

Horny L, Chlup H, Zitny R, Vonavkova T, Vesely J, Lanzer P (2012). *Ex Vivo* Coronary Stent Implantation Evaluated with Digital Image Correlation. Exp Mech 52(9): 1555–1558. DOI: 10.1007/s11340-012-9620-6.

Horný L, Roubalová L, Kronek J, Chlup H, Adámek T, Blanková A, et al. (2022b). Correlation between age, location, orientation, loading velocity and delamination strength in the human aorta. J Mech Behav Biomed Mater 133: 105340. DOI: 10.1016/j.jmbbm.2022.105340.

Jiang M, Lawson ZT, Erel V, Pervere S, Nan T, Robbins AB, et al. (2020). Clamping soft biologic tissues for uniaxial tensile testing: A brief survey of current methods and development of a novel clamping mechanism. J Mech Behav Biomed Mater 103: 103503. DOI: 10.1016/j.jmbbm.2019.103503.

Karimi A, Navidbakhsh M, Shojaei A (2015). A combination of histological analyses and uniaxial tensile tests to determine the material coefficients of the healthy and atherosclerotic human coronary arteries. Tissue Cell 47(2): 152–158. DOI: 10.1016/j.tice.2015.01.004.

Karimi A, Navidbakhsh M, Shojaei A, Faghihi S (2013). Measurement of the uniaxial mechanical properties of healthy and atherosclerotic human coronary arteries. Mater Sci Eng C Mater Biol Appl 33(5): 2550–2554. DOI: 10.1016/j.msec.2013.02.016.

Kobayashi T, Kurazumi H, Sato M, Gohra H (2018). Pseudoaneurysm rupture after acute Type A dissection repair: possible reaction to BioGlue. Interact Cardiovasc Thorac Surg 26(2): 331–332. DOI: 10.1093/icvts/ivx331.

Ma WG, Ziganshin BA, Guo CF, Zafar MA, Sieller RS, Tranquilli M, Elefteriades JA (2017). Does BioGlue contribute to anastomotic pseudoaneurysm after thoracic aortic surgery? J Thorac Dis 9(8): 2491–2497. DOI: 10.21037/jtd.2017.06.120.

Petuchova A, Maknickas A, Kostenko E, Stonkus R (2023). Experimental and theoretical investigation of aortic wall tissue in tensile tests. Technol Health Care 31(6): 2411–2421. DOI: 10.3233/THC-235007.

Pratali S, Milano A, Codecasa R, De Carlo M, Borzoni G, Bortolotti U (2000). Improving hemostasis during replacement of the ascending aorta and aortic valve with a composite graft. Tex Heart Inst J 27(3): 246–249.

Razzouk A, Gundry S, Wang N, Heyner R, Sciolaro C, Van Arsdell G, et al. (1993). Pseudoaneurysms of the aorta after cardiac surgery or chest trauma. Am Surg 59(12): 818–823.

Rečičárová S, Chlup H, Jonák M, Netuka I (2023a). False aneurysms of the thoracic aorta: anastomosis investigation using the inflation-extension test. J Appl Biomed 21(4): 174–179. DOI: 10.32725/jab.2023.023.

Rečičárová S, Ivák P, Pirk J (2023b). Surgical management of ascending aorta pseudoaneurysm in a patient with COVID-19. Cor Vasa 65(1): 113–115. DOI: 10.33678/cor.2022.060.

Recicarova S, Jonak M, Netuka I (2024). Comprehensive multimodality treatment of thoracic aorta pseudoaneurysms: a single-center experience. Gen Thorac Cardiovasc Surg 72(6): 387–394. DOI: 10.1007/s11748-023-01986-9.

Rubio Alvarez J, Sierra Quiroga J, Martinez de Alegria A, Delgado Dominguez C (2011). Pulmonary embolism due to biological glue after repair of type A aortic dissection. Interact Cardiovasc Thorac Surg 12(4): 650–651. DOI: 10.1510/icvts.2010.261933.

Schlatmann TJM, Becker AE (1977). Histologic changes in the normal aging aorta: Implications for dissecting aortic aneurysm. Am J Cardiol 39(1): 13–20. DOI: 10.1016/S0002-9149(77)80004-0.

Scholze M, Safavi S, Li KC, Ondruschka B, Werner M, Zwirner J, Hammer N (2020). Standardized tensile testing of soft tissue using a 3D printed clamping system. HardwareX 8: e00159. DOI: 10.1016/j.ohx.2020.e00159.

Spacek M, Chlup H, Mitas P, Vesely J, Lambert L, Mlcek M, et al. (2019). Three-layer collagen-based vascular graft designed for low-flow peripheral vascular reconstructions. J Appl Biomed 17(1): 47–52. DOI: 10.32725/jab.2019.002.

Spittell JA, Jr. (1983). Hypertension and arterial aneurysm. J Am Coll Cardiol 1(2 Pt 1): 533–540. DOI: 10.1016/S0735-1097(83)80085-0.

Straka F, Schornik D, Masin J, Filova E, Mirejovsky T, Burdikova Z, et al. (2017). A New Approach to Heart Valve Tissue Engineering Based on Modifying Autologous Human Pericardium by 3D Cellular Mechanotransduction. J Biomater Tissue Eng 7(7): 527–543. DOI: 10.1166/jbt.2017.1598.

Straka F, Schornik D, Masin J, Filova E, Mirejovsky T, Burdikova Z, et al. (2018). A human pericardium biopolymeric scaffold for autologous heart valve tissue engineering: cellular and extracellular matrix structure and biomechanical properties in comparison with a normal aortic heart valve. J Biomater Sci Polym Ed 29(6): 599–634. DOI: 10.1080/09205063.2018.1429732.

Sugita S, Matsumoto T (2013). Novel biaxial tensile test for studying aortic failure phenomena at a microscopic level. Biomed Eng Online 12: 3. DOI: 10.1186/1475-925X-12-3.

Šupová M, Suchý T, Chlup H, Šulc M, Kotrč T, Šilingová L, et al. (2023). The electron beam irradiation of collagen in the dry and gel states: The effect of the dose and water content from the primary to the quaternary levels. Int J Biol Macromol 253(Pt 4): 126898. DOI: 10.1016/j.ijbiomac.2023.126898.

Takada J, Hamada K, Zhu X, Tsuboko Y, Iwasaki K (2023). Biaxial tensile testing system for measuring mechanical properties of both sides of biological tissues. J Mech Behav Biomed Mater 146: 106028. DOI: 10.1016/j.jmbbm.2023.106028.

Veselý J, Horný L, Chlup H, Adámek T, Krajíček M, Žitný R (2015). Constitutive modeling of human saphenous veins at overloading pressures. J Mech Behav Biomed Mater 45: 101–108. DOI: 10.1016/j.jmbbm.2015.01.023.

Witter K, Tonar Z, Matejka VM, Martinca T, Jonák M, Rokosný S, Pirk J (2010). Tissue reaction to three different types of tissue glues in an experimental aorta dissection model: a quantitative approach. Histochem Cell Biol 133(2): 241–259. DOI: 10.1007/s00418-009-0656-3.

Zia AW, Liu R, Wu X (2022). Structural design and mechanical performance of composite vascular grafts. Biodes Manuf 5(4): 757–785. DOI: 10.1007/s42242-022-00201-7.